Electronic Supplementary Information

Directing oxygen reduction reaction selectivity towards hydrogen peroxide *via* electric double layer engineering

Jingyi Chen,[1] Yilin Zhao,[1] Haozhou Yang,[1] Tianyu Zhang,[1] Lei Fan,[1] Chunfeng Li,[1] Lei Wang[1, 2] *

[1] Department of Chemical and Biomolecular Engineering, National University of Singapore (Singapore), E5, 4 Engineering Drive 4, Singapore 117585

[2] Centre for Hydrogen Innovations, National University of Singapore (Singapore), E8, 1 Engineering Drive 3, Singapore 117580

E-mail: wanglei8@nus.edu.sg

Experimental procedures

Chemicals: Cobalt(II) phthalocyanine (CoPc, 97%), iron(II) phthalocyanine (FePc, 90%), cetyltrimethylammonium bromide (CTAB, 98%), tetraoctylammonium bromide (TOAB, 98%), potassium hydroxide (KOH, 99.99%) and Nafion (5%) were purchased from Sigma-Aldrich. Lithium hydroxide (LiOH, 98%), N,N-Dimethylformamide (DMF, 99.5%) were purchased from Tokyo Chemical Industry (TCI). Cabot XC-72R carbon black was purchased from Suzhou Sinero Technology Co., Ltd. 20% Pt on Vulcan XC-72 (Pt/C) was purchased from Premetek Co., Ltd. All reagents were used as received without further purification.

Synthesis of CoPc/C: 1 mg CoPc and 10 mg carbon black were dispersed in 15 mL N, N-dimethyl formamide (DMF) under rigorous magnetic stirring for 24 hours at room temperature. The products were separated via centrifugation at 9500 rpm for 10 min and washed with ethanol three times. Then the separated black powder was dried at 80 ℃ overnight.

Synthesis of FePc/C: 1 mg FePc and 10 mg carbon black were dispersed in 15 mL N, N-dimethyl formamide (DMF) under rigorous magnetic stirring for 24 hours at room temperature. The products were separated via centrifugation at 9500 rpm for 10 min and washed with ethanol three times. Then the separated black powder was dried at 80 ℃ overnight.

Materials characterization: Transmission electron microscopy (TEM) and corresponding energy-dispersive X-ray spectroscopy (EDS) were taken by a JEOL JEM-2010F TEM. Scanning electron microscope (SEM) and corresponding energy-dispersive X-ray spectroscopy (EDS) were carried by JEOL JSM-7610F SEM. X-ray diffraction (XRD) patterns were recorded on a Bruker D8-advance X-ray powder diffractometer with CuKα radiation (λ=1.5406 Å). X-ray photoelectron

spectroscopy (XPS) was conducted on Kratos Axis Ultra^{DLD} (Mono Al Kα, hν= 1486.71 eV). Fourier-transform infrared spectroscopy (FTIR) was recorded using VERTEX 70 FT-IR Spectrometer.

Electrochemical measurements: All of the electrochemical performance measurements were performed using CHI760e electrochemical workstation with a typical three-electrode system. An Hg/HgO electrode and a graphite rod electrode were used as reference electrode and counter electrode, respectively. All measured potentials were converted to reversible hydrogen electrode (RHE) scale based on:

$$E\ vs.RHE = E\ vs.Hg/HgO + 0.098 + 0.0592 * pH$$

pH value of 13 was measured for electrolytes with different CTAB concentrations using pH meter (LAQUA PH1300). A rotating ring-disk electrode set-up (RRDE-3A, ALS Co., Ltd) containing a glassy carbon disk electrode and a platinum ring served as the working electrode. The collection efficiency (N) of RRDE electrode was calibrated using ferrocyanide/ferricyanide in the electrolyte containing 0.1 M KOH and 10 mM $K_3Fe(CN)_6$ (Fig. S8). LSV was conducted with the rotation rate from 400 rpm to 1600 rpm, with E_{ring} = 1.55 V and a sweep rate of 20 mV/s. The catalyst ink was prepared by dispersing 1 mg catalyst and 10 uL Nafion in 190 μL mixture of isopropanol (122 μL) and water (68 μL). The ink was further sonicated for 30 minutes and then loaded 7.5 μL on glassy carbon disk electrode to reach the loading of around 0.3 mg/cm^2. 0.1 M KOH with different concentrations of CTAB was used as electrolyte.

The ORR performance measurement was conveyed in O_2-saturated electrolyte. LSV was performed at the scan rate of 10 mV/s and 1600 rpm, with E_{ring} =1.48 V. Stability test was carried out using i-t technique in O_2-saturated 0.1 M KOH + 2 mM CTAB. The decrease of ring current was caused by ring oxidation under

applied E_{ring} and continuous test. Rapid cyclic voltammetry was applied on Pt ring to remove Pt oxides.

H_2O_2 molar fraction (H_2O_2%) and electron transfer number (n) were calculated based on:

$$H_2O_2\ molar\ fraction = 100 * \frac{2I_R/N}{I_D + I_R/N}$$

$$n = \frac{4I_D}{I_D + I_R/N}$$

I_D is disk current,

I_R is ring current,

and N is calibrated collection efficiency of RRDE.

Current deconvolution was analyzed based on:

$$j_{O2P} = j_D \frac{\theta N + 1}{2\theta N}$$

$$\theta = \left|\frac{j_D}{j_R}\right|$$

$$j_{P2H} = j_D - j_{O2P}$$

Where j_{O2P} is current density for oxygen reduction to peroxide,

j_{P2H} is current density for peroxide reduction to hydroxide,

j_D is disk current density,

and j_R is ring current density.

Kinetics current density (j_K) was fitted based on Koutecky–Levich (K-L) equation:

$$\frac{1}{j} = \frac{1}{j_L} + \frac{1}{j_K} = \frac{1}{B\omega^{1/2}} + \frac{1}{j_K}$$

$$B = 0.62nFAC_0{D_0}^{2/3}\mu^{-1/6}$$

j is the measured current density,

j_L and j_K are diffusion-limiting current density and kinetic current density,

ω is angular velocity (rad/s),

n is electron transfer number,

F is Faradic constant (96485 C/mol),

A is disk electrode area,

C_0 is saturated O_2 bulk concentration in electrolyte,

D_0 is O_2 diffusion coefficient,

And μ is electrolyte kinematic viscosity.

Oxygen uptake rate (ν_{O_2}) was calculated based on:

$$\nu_{O_2} = \left[\frac{FE(H_2O_2) * j_D}{2} + \frac{[1 - FE(H_2O_2)] * j_D}{4}\right] \div 96485$$

$$FE(H_2O_2) = \frac{I_R/N}{I_D} * 100\%$$

C_{dl} calculation:

$$C_{dl} = \frac{(CPE \cdot R_{ct})^{1/n}}{R_{ct}}$$

Gouy−Chapman−Stern (GCS) model:

$$\frac{1}{C_{dl}} = \frac{1}{C_H} + \frac{1}{C_D}$$

C_{dl} is double layer capacitance. C_H and C_D are the capacitance of compact layer and diffusion layer, respectively.

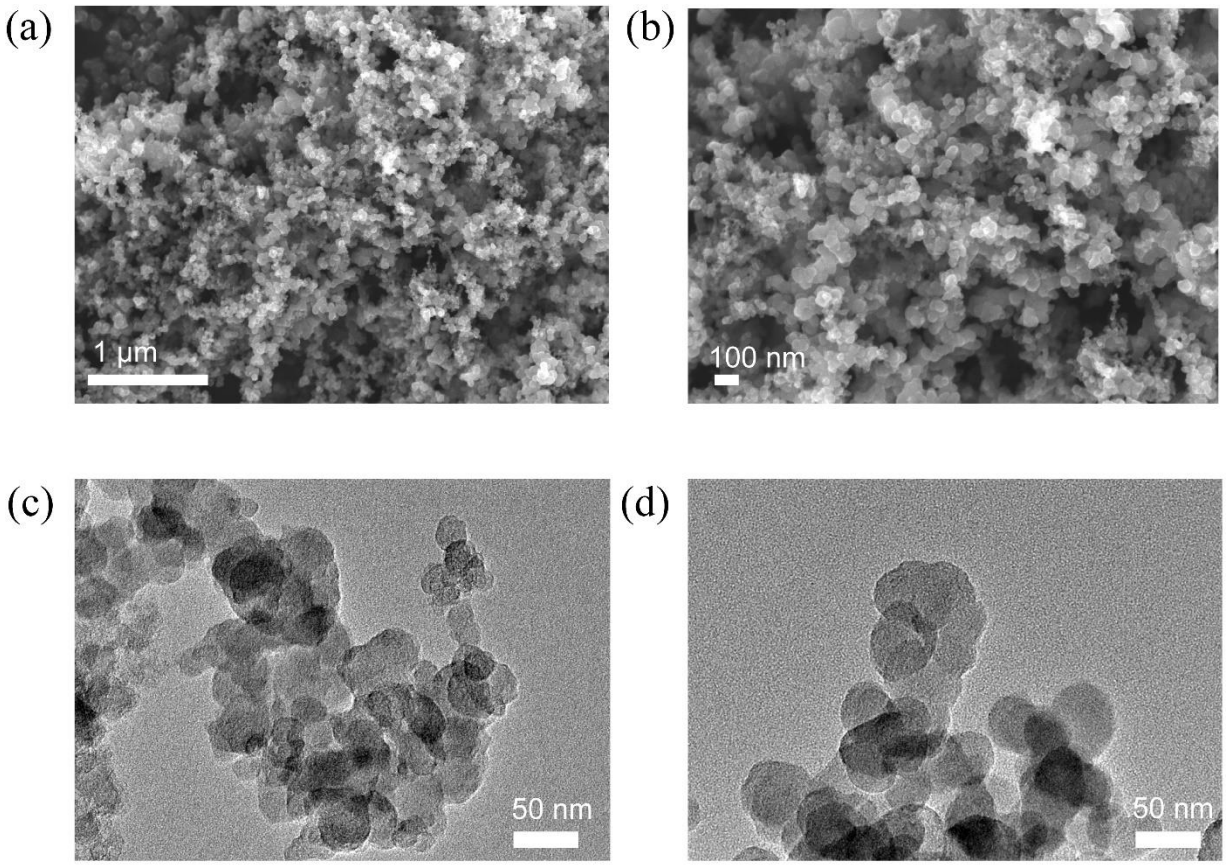

Fig S1. SEM images (a, b) and TEM images (c, d) of XC-72R carbon black.

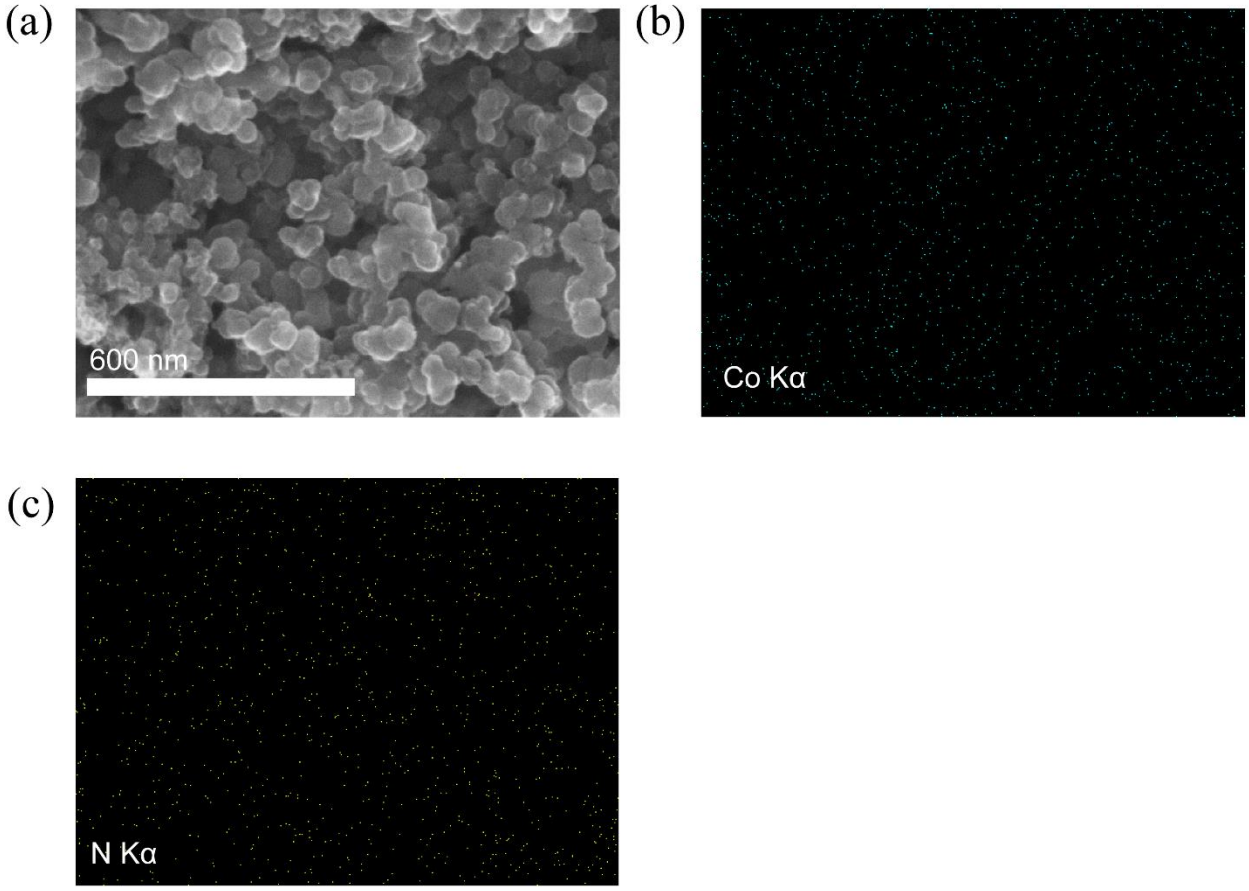

Fig. S2. SEM images (a) and corresponding EDX mapping of CoPc/C (b, c).

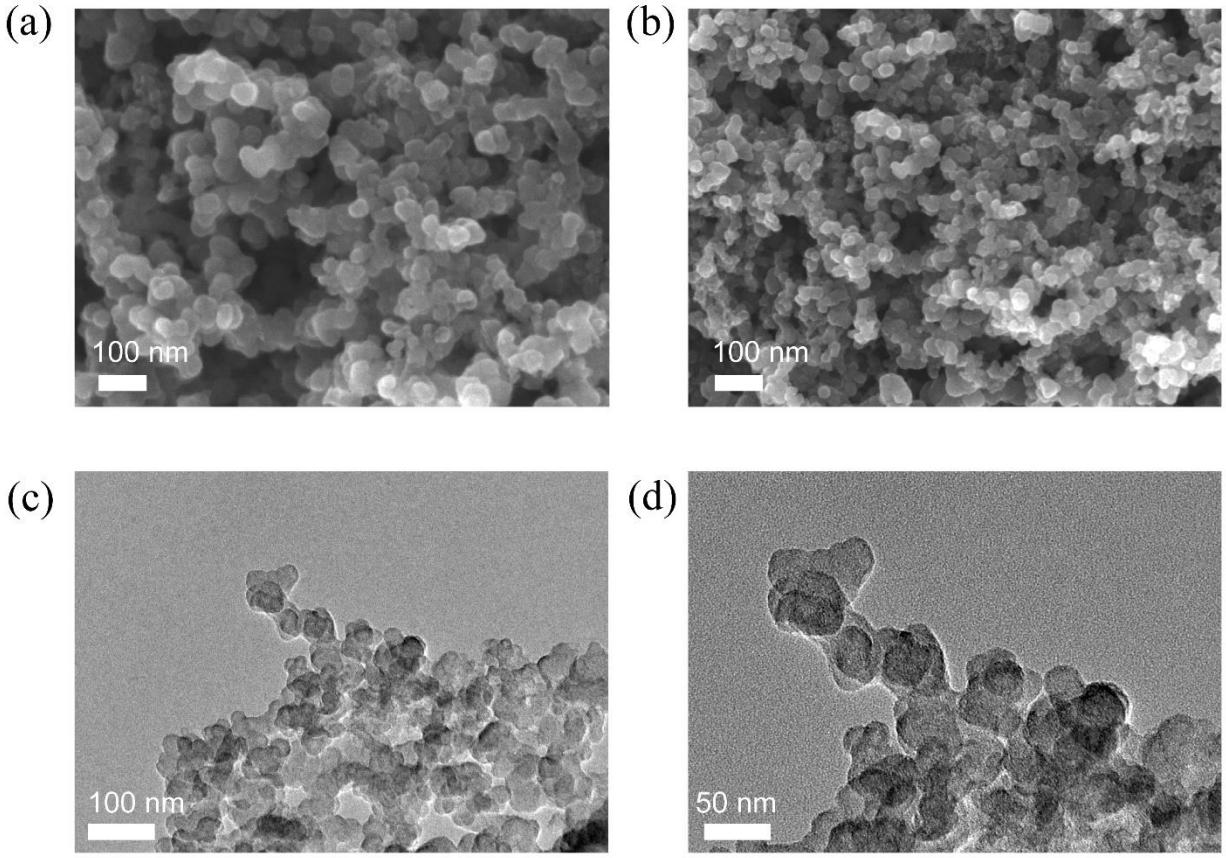

Fig. S3. SEM images (a, b) and TEM images (c, d) of post-reaction catalyst.

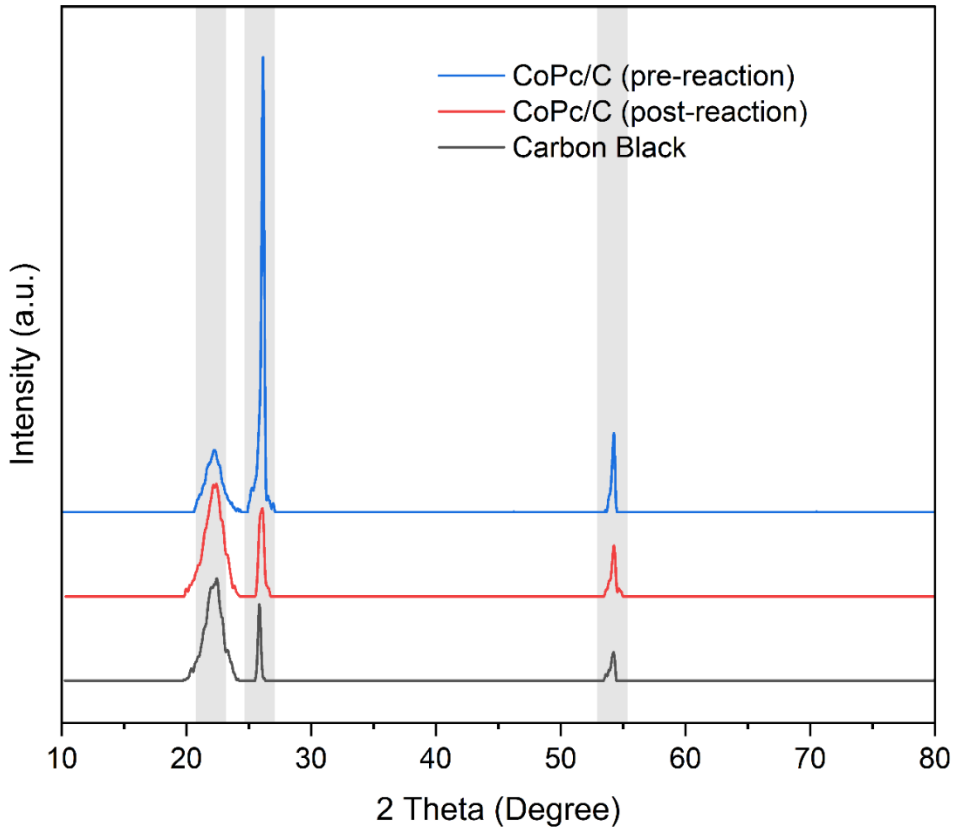

Fig. S4. XRD of CoPc/C (as synthesized and post-reaction) and carbon black.

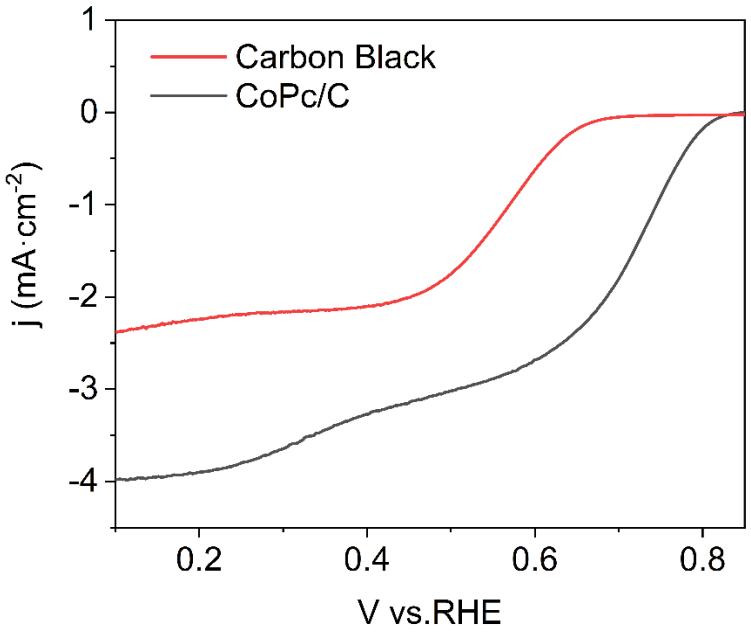

Fig. S5. ORR performance of carbon black and CoPc/C in O_2-saturated 0.1 M KOH on RRDE at 1600 rpm.

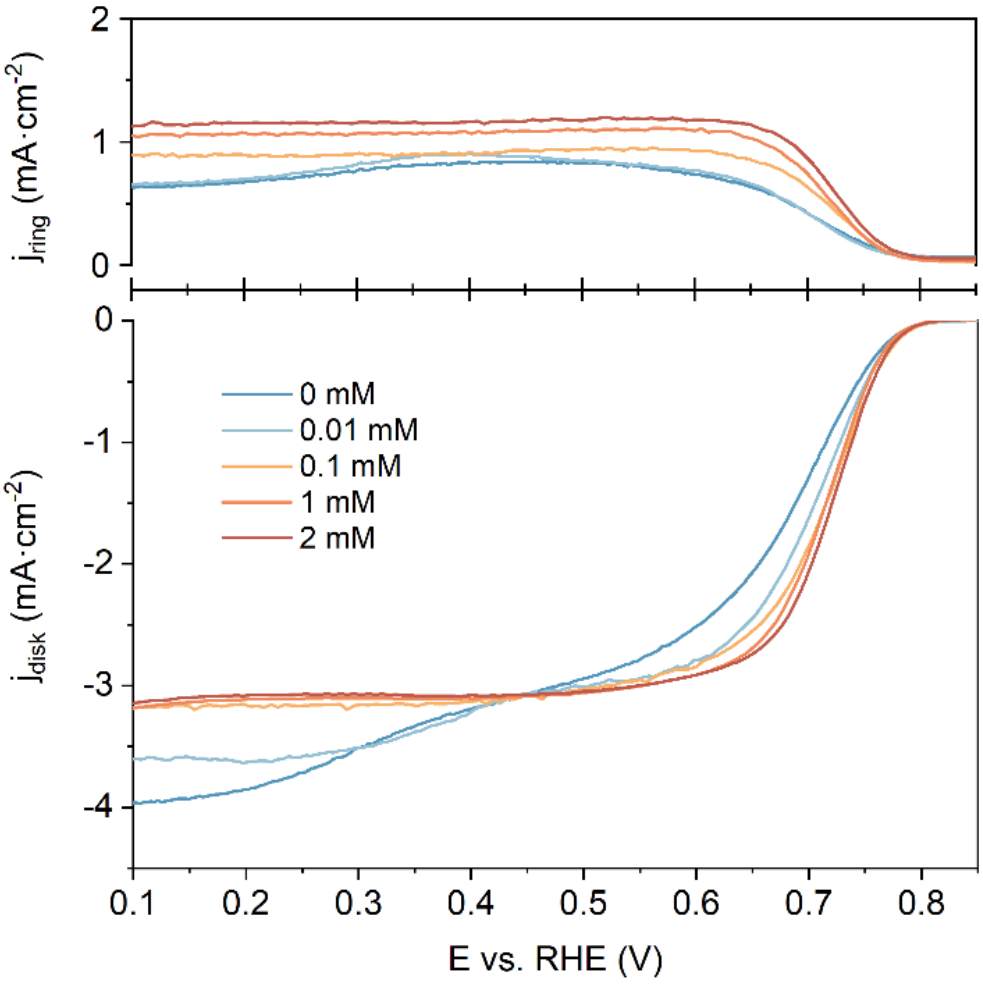

Fig. S6. ORR performance of CoPc/C in O_2-saturated 0.1 M KOH with different CTAB concentrations on RRDE at 1600 rpm.

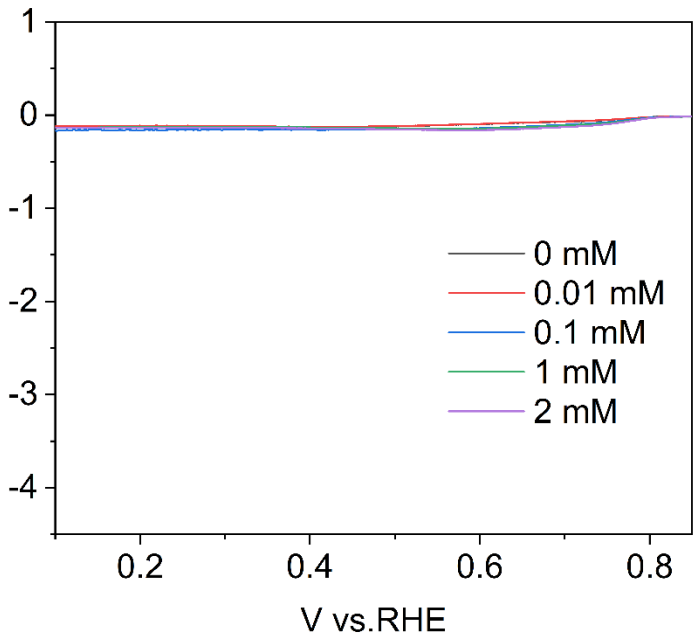

Fig. S7. ORR performance of CoPc/C in N_2-saturated 0.1 M KOH with different CTAB concentrations on RRDE at 1600 rpm.

(a)

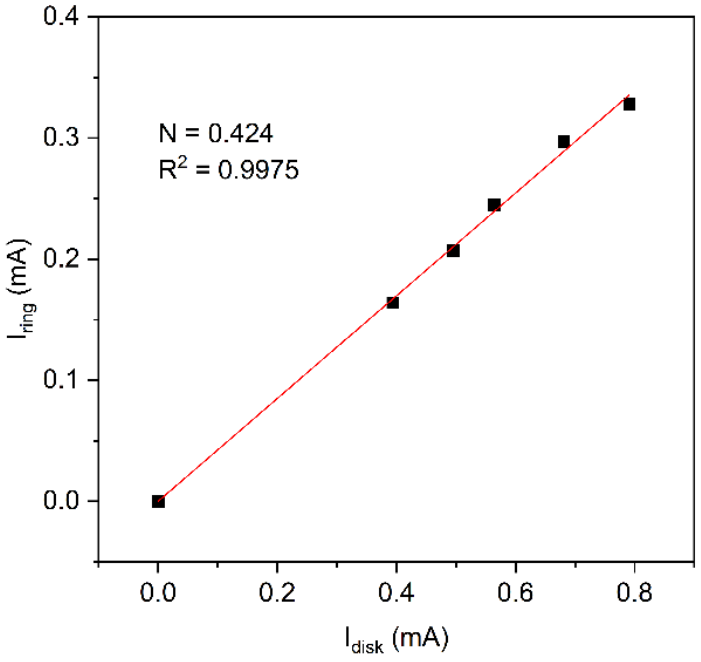

(b)

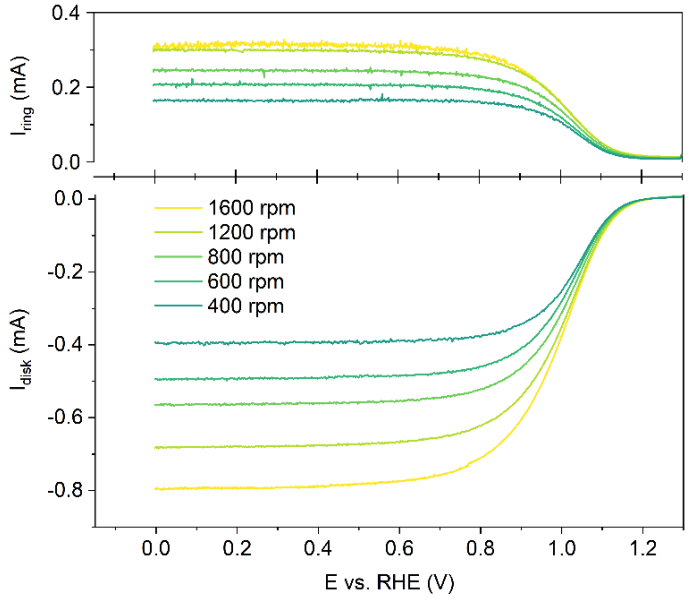

Fig. S8. RRDE collection efficiency calibration in 0.1 M KOH with 10 mM $K_3Fe(CN)_6$.

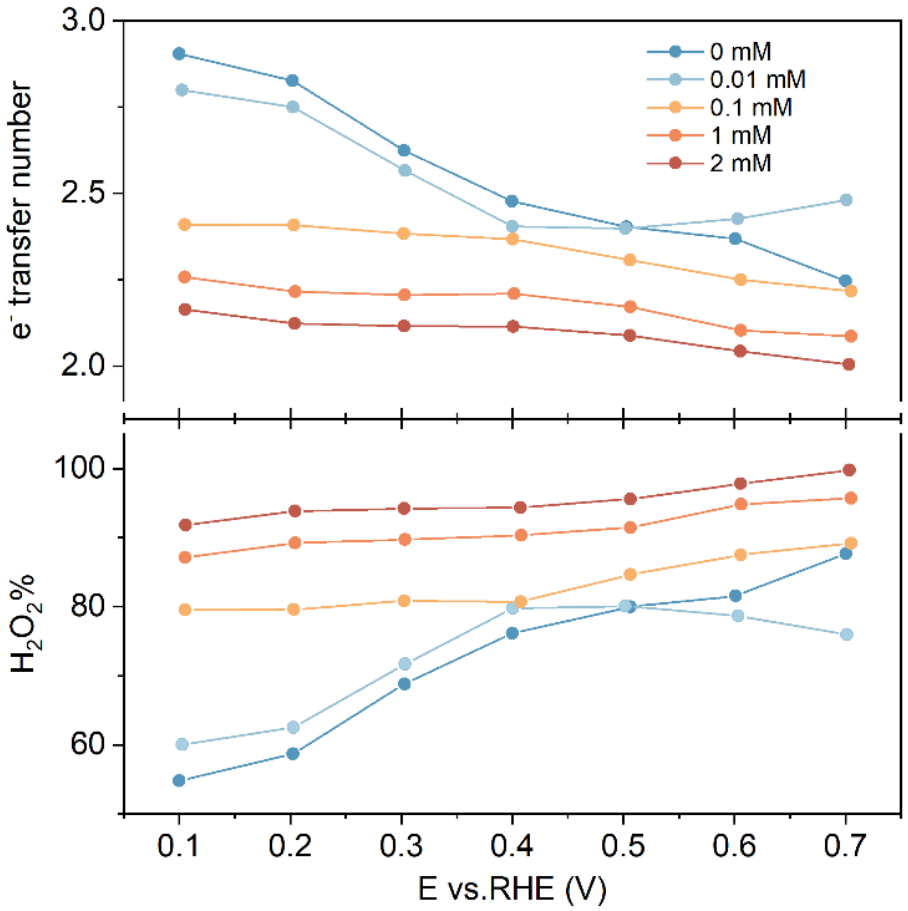

Fig. S9. Calculated H_2O_2 molar fraction and electron transfer number of CoPc/C in O_2-saturated 0.1 M KOH with different CTAB concentrations on RRDE at 1600 rpm.

(a)

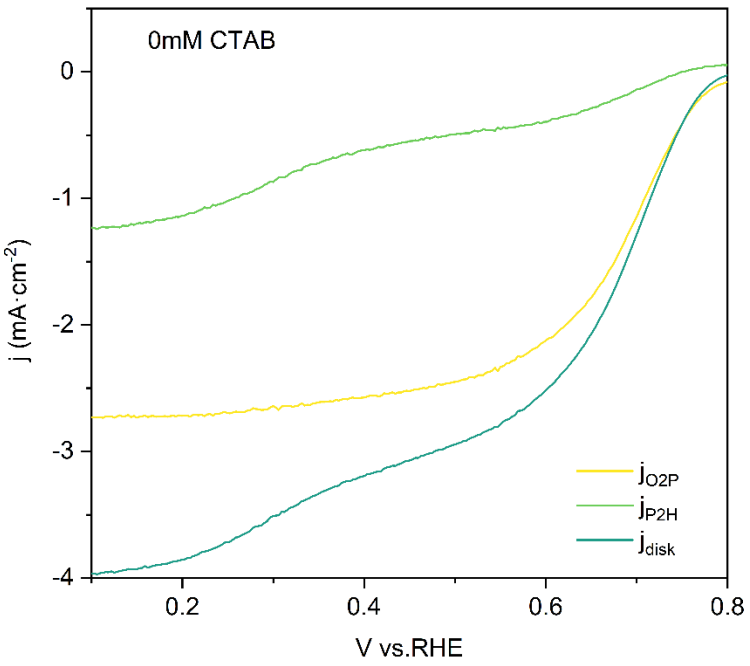

(b)

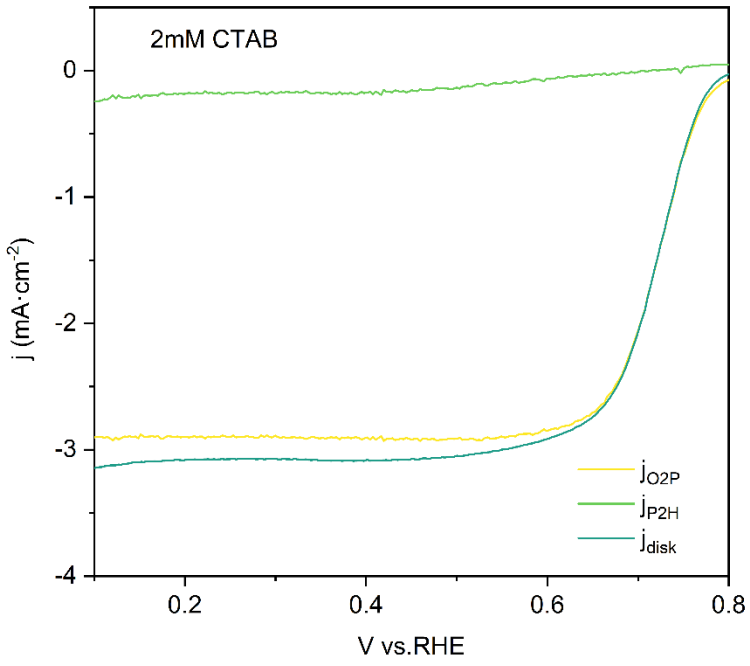

Fig. S10. ORR current deconvolution of CoPc/C in 0.1 M KOH (a) and 0.1 M KOH + 2 mM CTAB (b). j_{O2P} is current density for oxygen reduction to peroxide, and j_{P2H} is current density for peroxide reduction to hydroxide.

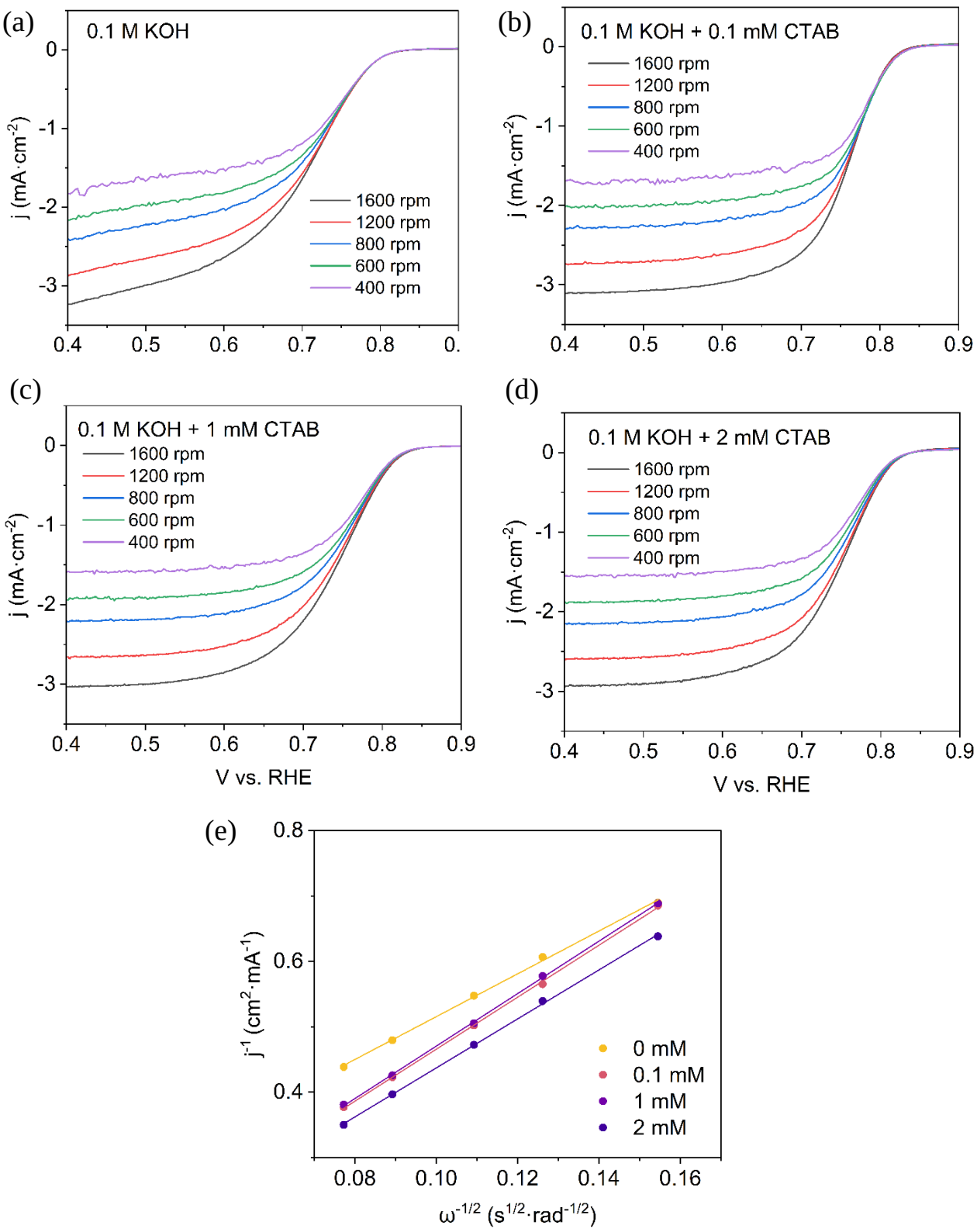

Fig. S11. LSV at different rotating speed (a-d) and K-L plots at 0.76 V (e) of CoPc/C in 0.1M KOH with various CTAB concentrations.

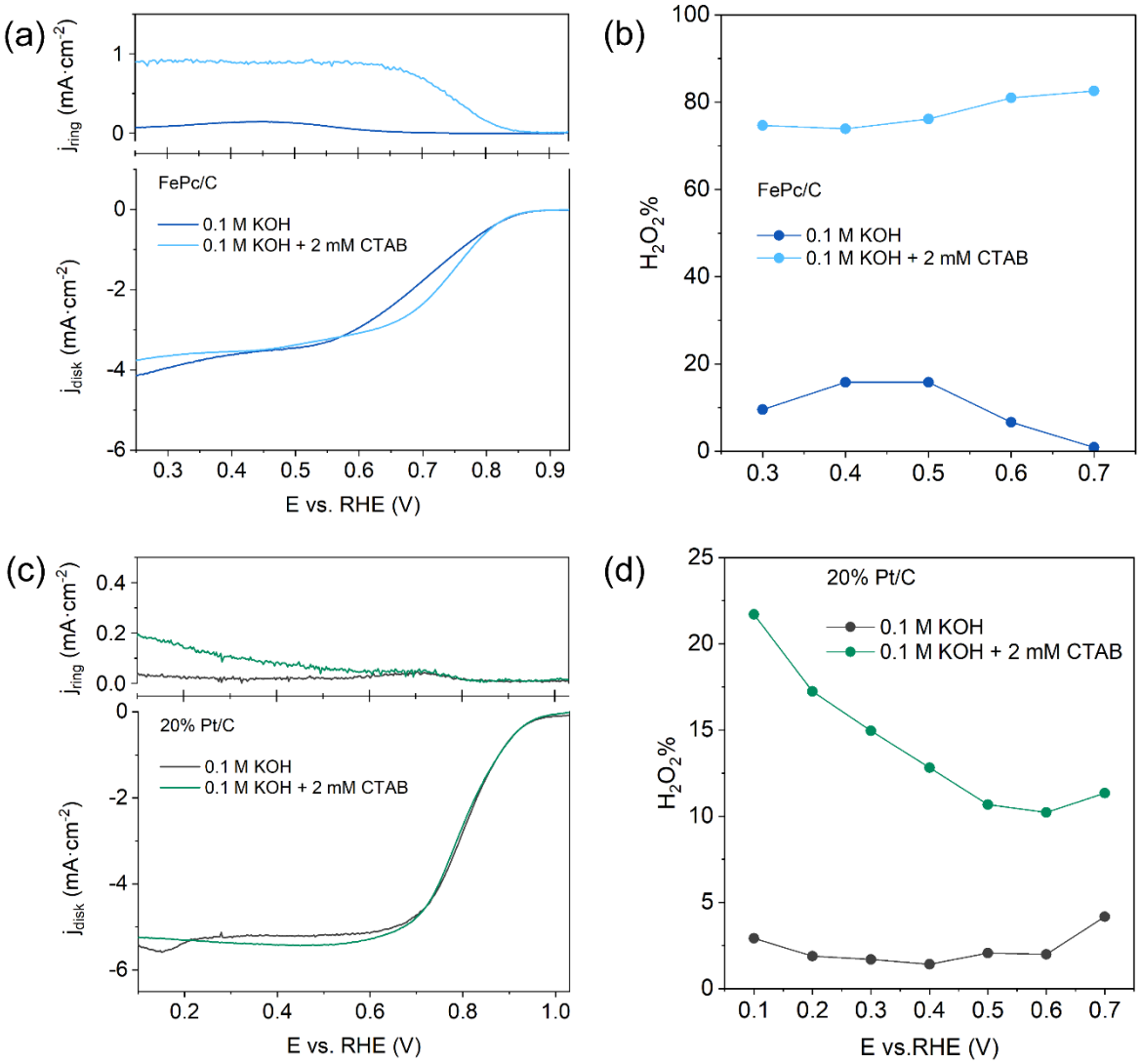

Fig. S12. (a) LSV at 1600 rpm and (b) H_2O_2 selectivity of FePc/C in O_2-saturated 0.1 M KOH with or without 2 mM CTAB. (c) LSV at 1600 rpm and (d) H_2O_2 selectivity of 20% Pt/C in O_2-saturated 0.1 M KOH with or without 2 mM CTAB.

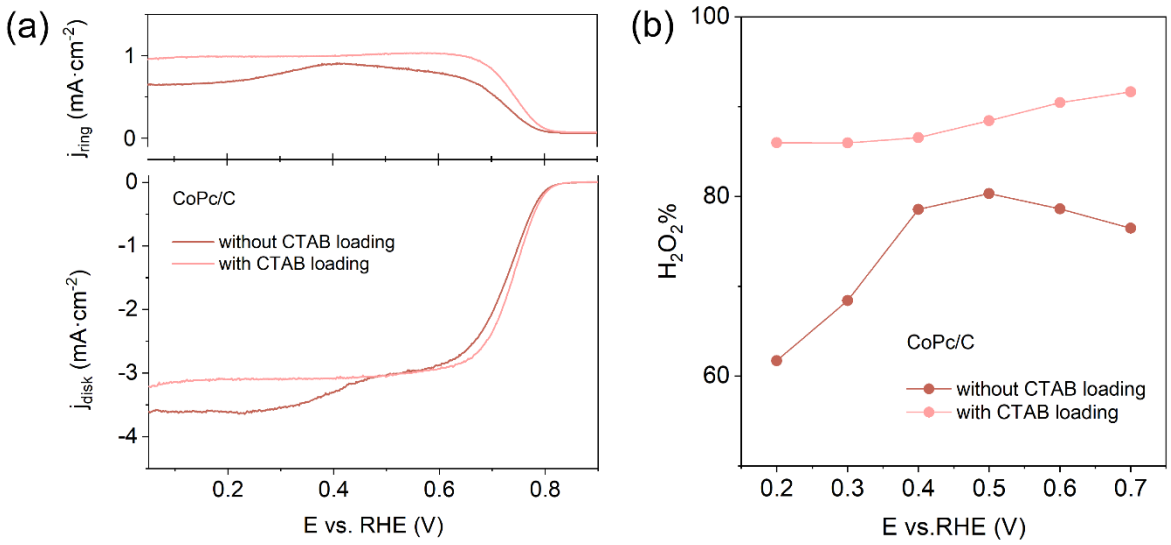

Fig. S13. (a) LSV at 1600 rpm and (b) H_2O_2 selectivity of CoPc/C in O_2-saturated 0.1 M KOH with or without CTAB loading on catalyst. Specifically, for the sample with CTAB loading, 25 mg CTAB was dissolved in 200 μL ink (10 uL Nafion + 122 μL isopropanol + 68 μL water) and mixed with 1mg CoPc/C.

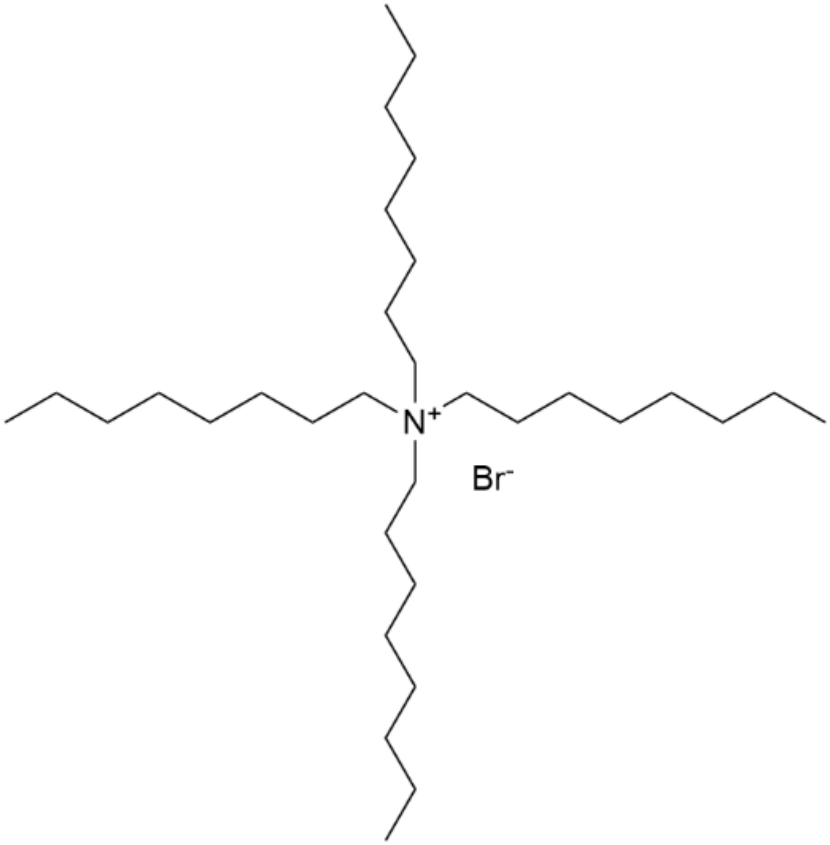

Fig. S14. Structure of Tetraoctylammonium bromide (TOAB).

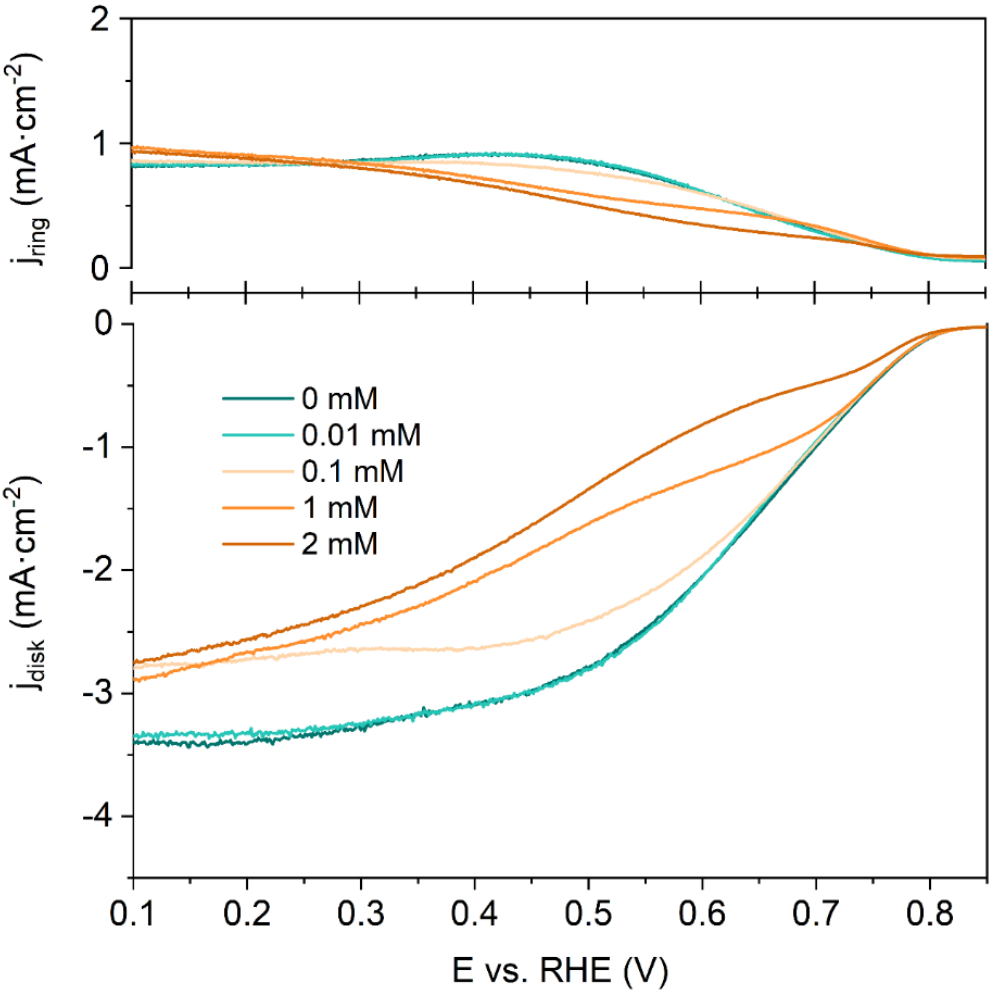

Fig. S15. ORR performance of CoPc/C in O_2-saturated 0.1 M KOH with different TOAB concentrations on RRDE at 1600 rpm.

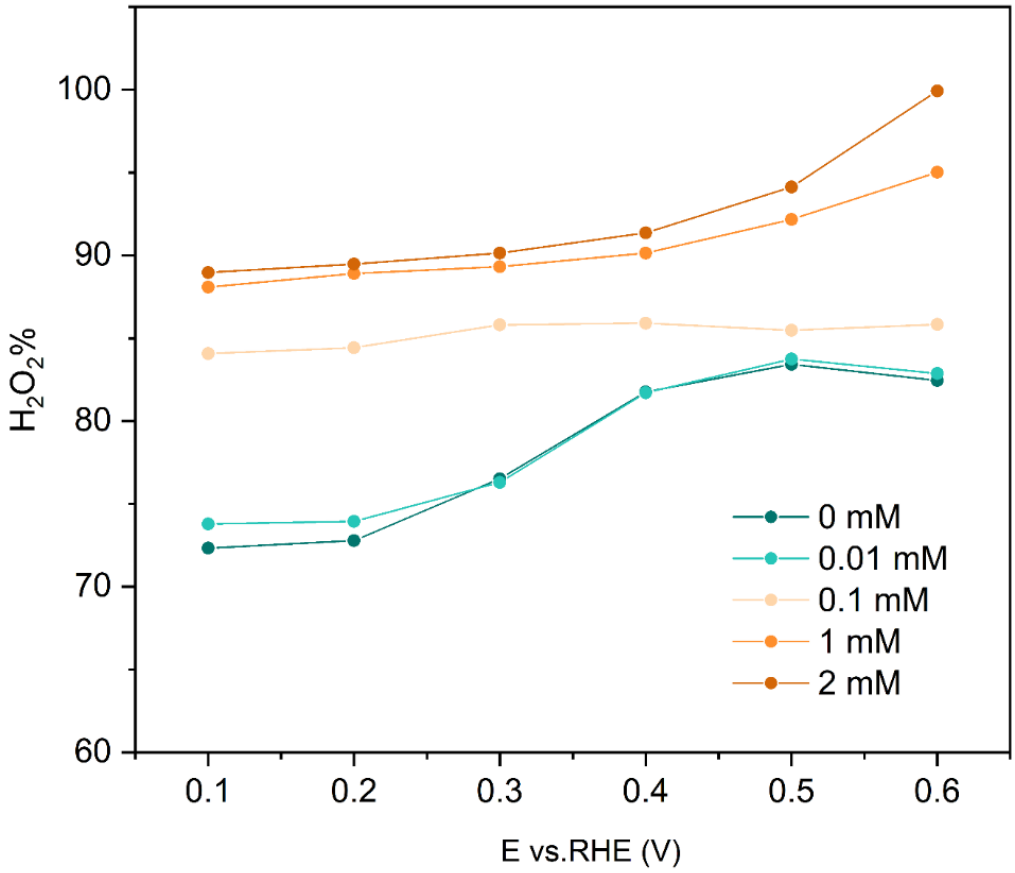

Fig. S16. Calculated H_2O_2 molar fraction of CoPc/C in O_2-saturated 0.1 M KOH with different TOAB concentrations on RRDE at 1600 rpm.

(a)

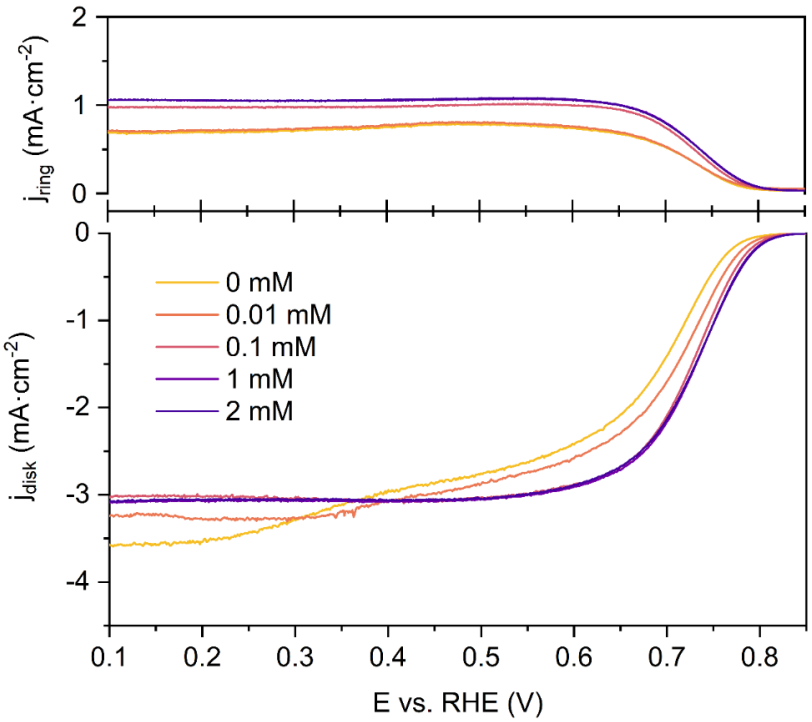

(b)

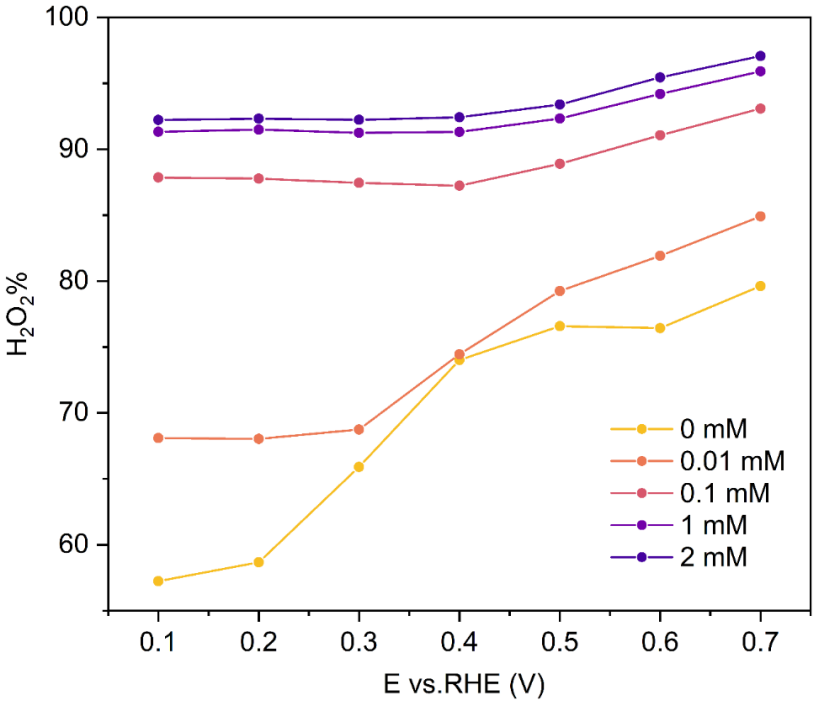

Fig. S17. ORR performance (a) and calculated H_2O_2 molar fraction (b) in O_2-saturated 0.1 M LiOH of CoPc/C with different CTAB concentrations on RRDE at 1600 rpm.

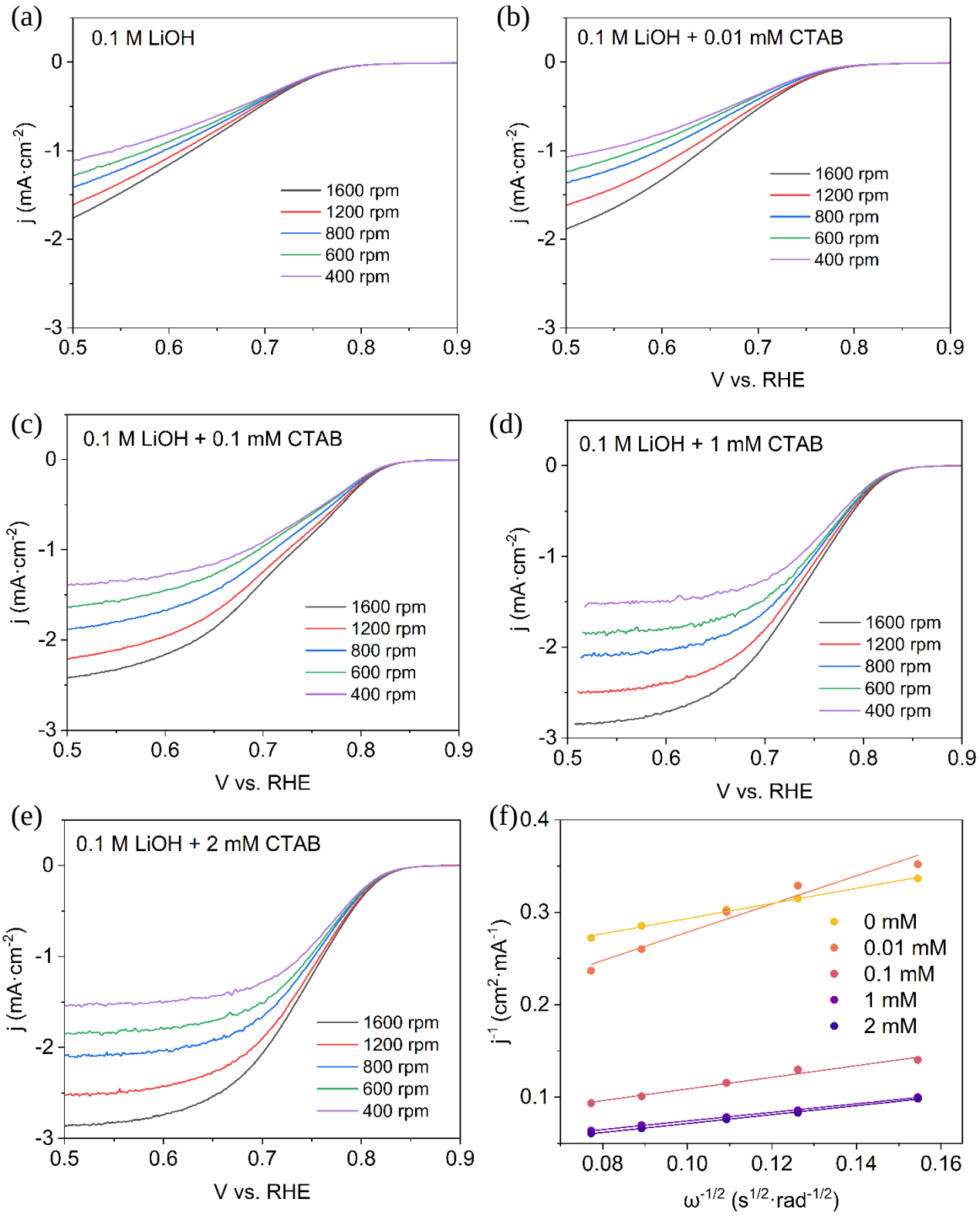

Fig. S18. LSV at different rotating speed (a-e) and K-L plots at 0.72 V (f) of CoPc/C in 0.1M LiOH with various CTAB concentrations.

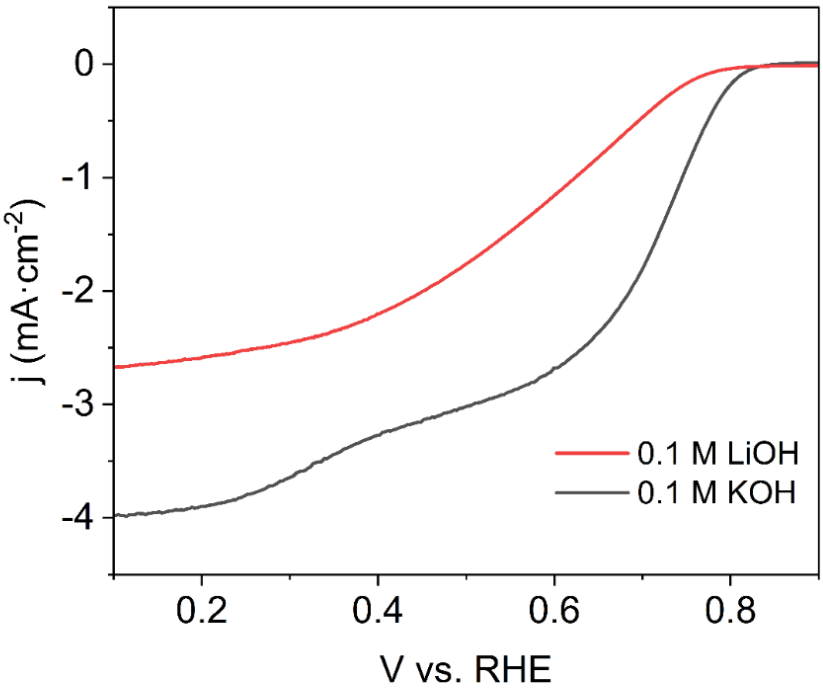

Fig. S19. ORR performance of CoPc/C in O_2-saturated 0.1 M LiOH and KOH at 1600 rpm.

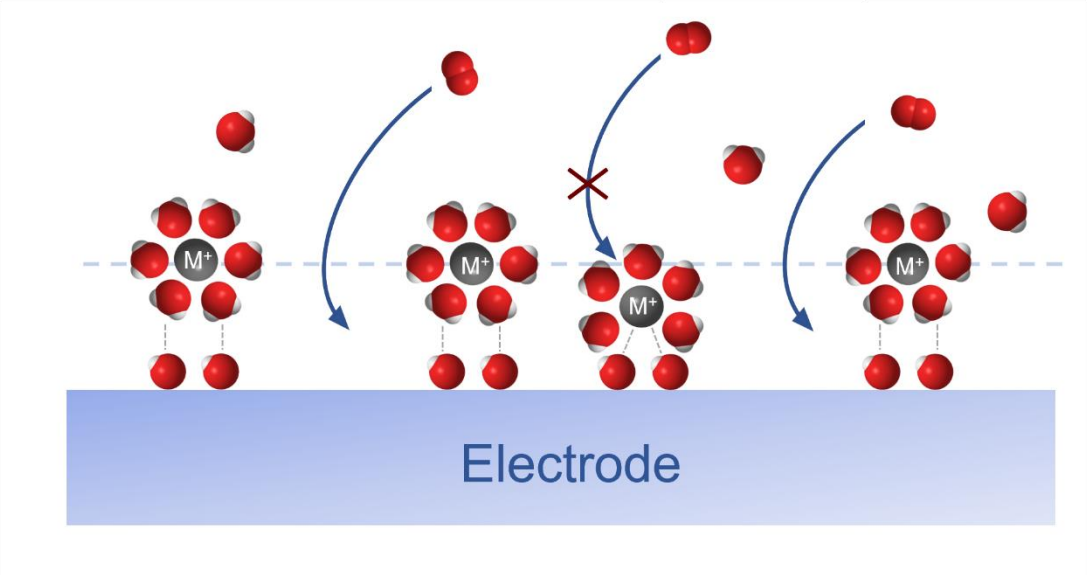

Fig. S20. Illustration of hindered oxygen accessibility towards active sites caused by the formation of OH_{ad}–$M^{+}(H_2O)_x$ clusters. Red, oxygen; white, hydrogen; grey, carbon.

Table S1. Linear fitting information for k-l plots in 0.1 M KOH

Linear fitting information / CTAB conc. (mM)	R square	Slope ($mV \cdot dec^{-1}$)	Intercept (mV)
0	0.99859	3.27141	0.18837
0.1	0.99948	3.97282	0.06847
1	0.99976	4.00891	0.06963
2	0.99943	3.74302	0.06286

Table S2. Linear fitting information for Tafel slope

Linear fitting information / CTAB conc. (mM)	R square	Slope ($mV \cdot dec^{-1}$)	Intercept (mV)
0	0.99803	-0.05658	0.76441
0.01	0.99778	-0.05757	0.76342
0.1	0.99265	-0.06024	0.76849
1	0.99887	-0.05349	0.7664
2	0.99731	-0.05514	0.77003

Table S3. Electrochemical impedance spectroscopy fitting results

Fitted data / CTAB conc.	R_s (ohm)	R_{ct} (ohm)	CPE-T (μF)	CPE-P
0	8.195	206.7	$2.7753*10^{-2}$	0.87626
0.1	2.553	125.5	$4.4139*10^{-2}$	0.88429
1	6.752	106.5	$2.6302*10^{-2}$	0.93082
2	5.227	103.4	$4.205*10^{-2}$	0.90029

(Fitted by Zview2 software)

Table S4. Linear fitting information for k-l plots in 0.1 M LiOH

Linear fitting information / CTAB conc. (mM)	R square	Slope ($mV \cdot dec^{-1}$)	Intercept (mV)
0	0.99521	0.82007	0.21121
0.01	0.96472	1.52751	0.1257
0.1	0.97927	0.63053	0.04575
1	0.99905	0.465	0.0277
2	0.9984	0.48381	0.02296